AIMS Materials Science, 4(1): 209-222.
DOI:10.3934/matersci.2017.1.209
Received: 20 October 2016
Accepted: 10 January 2017
Published: 25 January 2017

http://www.aimspress.com/journal/Materials

Research article

The interactions between CdTe quantum dots and proteins: understanding nano-bio interface

Shreeram S. Joglekar [1], Harish M. Gholap [2], Prashant S. Alegaonkar [3], and Anup A. Kale [4,*]

[1] Department of Biosciences, Defence Institute of Advanced Technology, Pune-411025, India
[2] Department of Physics, Fergusson College, Pune-411005, Pune, India
[3] Department of Applied Physics, Defence Institute of Advanced Technology, Pune-411025, India
[4] Department of Applied Science, College of Engineering Pune, Pune-411005, India

* **Correspondence:** Email: aak.appsci@coep.ac.in; anupakale@gmail.com.

Abstract: Despite remarkable developments in the nanoscience, relatively little is known about the physical (electrostatic) interactions of nanoparticles with bio macromolecules. These interactions can influence the properties of both nanoparticles and the bio-macromolecules. Understanding this bio-interface is a prerequisite to utilize both nanoparticles and biomolecules for bioengineering. In this study, luminescent, water soluble CdTe quantum dots (QDs) capped with mercaptopropionic acid (MPA) were synthesized by organometallic method and then interaction between nanoparticles (QDs) and three different types of proteins (BSA, Lysozyme and Hemoglobin) were investigated by fluorescence spectroscopy at pH = 7.4. Based on fluorescence quenching results, Stern-Volmer quenching constant (K_{sv}), binding constant (K_q) and binding sites (n) for proteins were calculated. The results show that protein structure (e.g., globular, metalloprotein, etc.) has a significant role in Protein-Quantum dots interactions and each type of protein influence physicochemical properties of Quantum dots differently.

Keywords: protein; quantum dot; electrostatic interactions; fluorescence; Stern-Volmer; nano-bio interface

1. Introduction

Nanocrystals of semiconducting materials which are also known as quantum dots (QDs) have all three dimensions confined to the 2–15 nm length scale [1,2,3]. Quantum dots (QDs) have gained a lot of attention in the past decade. The quantum confinement of their electronic states makes them quite attractive, showing some unique optical properties such as high quantum yield, symmetrical emission spectra, broad-band excitation, photo stability, and readily tunable spectra [2,4,5,6] compared to conventional dyes. In recent decades, their applications in cell labeling [7] biomolecule detection [8], immune reaction analysis [5] and drug screening [9] have increased remarkably. When QDs are used as biomarkers, especially *in vivo* bio labeling, the interactions between certain small biomolecules in the bio system and the surface of QDs may influence the efficiency of the electron-hole recombination process, leading to luminescence change of the QDs [10].

Interactions between CdSe/ZnS QD and human serum albumin (HSA) [4], CdSe/ZnS QD and bovine serum albumin (BSA) [11], CdS QD and BSA [12], CdS QD and hemoglobin (Hb) [13], CdTe QD and HAS [14] and CdSe QD and Hb [15] have been reported. However, those studies only focus on the interaction of QDs with different proteins, but do not relate the interactions to the specific properties of proteins. The mechanism, which can be utilized to predict the binding of different proteins with QDs, is still obscure. Understanding the mechanism of interaction between nanoparticles and bio macromolecules is important to develop bioengineered nanoparticles as light emitting devices and labeling agents and therapeutic proteins.

Normal hemoglobin levels in blood are 12–16 g/dL in females & 14–18 g/dL in males. Human adult hemoglobin (HbA), A major protein component in erythrocytes is the tetramer of globin chains with two alpha and two beta subunits. The structure-functions relationships of hemoglobin are well-studied. The research on the interactions of Hb with other molecules such as dimethyl sulfoxide [16] anionic amphiphiles [17], Ln^{3+} ions [18], and hematoporphyrin [19] were limited though it is an important functional protein for reversible oxygen carrying and storage. The electrostatic adsorption of ultrafine inorganic particles, such as silica, zirconia, and titanium on Hb have been reported [20,21]. This work has examined the physical interactions between bovine Hb and CdTe QDs. The fluorescence quenching constant, binding constant, and conformational changes of Hb during the binding process are reported in the present paper.

Serum Albumin is the most abundant protein in blood plasma having reference level of 3.5–5.0 g/dL. It plays a key role in the transport of large number of metabolites, endogenous ligands, fatty acids, bilirubin, hormones, anesthetics and other commonly used drugs. Bovine serum albumin (BSA) has been one of the most extensively studied protein, particularly because of its structural homology with human serum albumin [14]. The BSA molecule is made up of three homologous domains (I, II, and III) which are divided into nine loops (L1–L9) by 17 disulfide bonds [22]. BSA has two tryptophans, Trp-134 and Trp-212 that possess intrinsic fluorescence, embedded in the first sub-domain IB and sub-domain IIA, respectively [23]. BSA is often used as coating reagent to modify the surface of nanoparticles due to its strong affinity towards a variety of nanoparticles, such as gold nanoparticles [24], silica nanoparticles [25], and QDs [26,27]. The BSA modified QDs have been applied to ion sensors [28,29], fluorescence resonance energy transfers (FRET) [13,30], and chemi-luminescence resonance energy transfer [31]. However, the mechanism of interaction between BSA and QDs has not yet been determined, which is often thought as an electrostatic attraction.

Lysozyme is a small monomeric non-globular protein found mostly in tears. The highest values

are seen in the age group of 21–40 years, and a decrease in lysozyme concentration observed with an increase in age from 30–40 years. The mean lysozyme content of tears is 1768 μg/ml in healthy subjects. Lysozyme consists of 129 amino acids containing α helix and β sheet domains with 4 disulphide bonds [32,33,34]. Lysozyme kills bacteria by rupturing their membrane structures. Lysozyme preferentially hydrolyses the β (1→4) glucosidic linkages between N-acetylmuramic acid and N-acetylglucosaminein the peptidoglycan in bacteria [35]. It is used in clinical practiceto treat inflammation, abcess, stomatitis & rheum etc. To further develop lysozyme as a therapeutic agent, the study of its interactions with nanopartilcesare crucial. Recently, interactions of lysozyme with CdTe QDs, TiO_2, SiO_2, ZnO and with silver nanoparticles were reported [36,37]. The focus of the study was to understand whether the conformational changes in proteins affect the fluorescence properties of quantum dots and proteins themselves. At the same time, it was interesting to observe how interactions with nanoparticles influence on the protein conformations.

2. Materials and Method

2.1. Synthesis of CdTe QDs

Cadmium chloride monohydrate ($CdCl_2 \cdot H_2O$), Tellurium powder (200 mesh), thioglycolic acid, 3-mercaptopropionic acid (MPA), Bovin Serum Albumin (BSA), Lysozyme (Lys) and Hemoglobin (Hb) were obtained from Sigma-Alderich. CdTe quantum dots capped with mercaptopropionicacid (MPA) were synthesized by organometallic route as reported by us earlier [38]. For CdTe quantum dot synthesis, NaHTe was used as the Te precursor and $CdCl_2$ as Cd precursor. The freshly prepared NaHTe solution was added to the N_2-saturated $CdCl_2$ solution containing MPA at pH = 9.0. The molar ratio of Cd^{2+}/Te^{2-}/MPA was 1:0.2:2.4. The solution was then heated and refluxed under nitrogen flow at 100 ºC with continuous stirring. Synthesis of nanoparticles was confirmed by UV-VIS spectroscopy, XRD and TEM.

2.2. Physical Interactions of QDs & Proteins

Interaction of the CdTe QDs & proteins were studied by fluorescence spectrophotometry at room temperature. The interactions between CdTe QDs (fix concentration of 3×10^{-7} M) and increasing concentrations of lysozyme (Lys), Bovine Serum Albumin (BSA), Hemoglobin (Hb) (10, 25, 50, 100, 200 μg/ml) werestudied in an aqueous solution. The fluorescence spectra were collected with excitation at 365 nm and intrinsic fluorescence spectra of CdTe QDs & proteins were recorded between 450 nm to 750 nm and 310 nm to 410 nm, respectively.

3. Results and Discussions

3.1. Spectral Characterization of CdTe QDs

The absorption spectrum of CdTe QDs shows a broad peak in visible region at 488 nm and the emission peak, λ_{Em} at 558 nm in Figure 1a, (the excitation wavelength, 365 nm). The emission spectrum of CdTe QDs is in good agreement with reported literature [39,40]. The absorption peak is well resolved, indicating narrow size distribution of the synthesized QDs. The Transmission Electron

Microscopy (TEM) images showed that the size of CdTe QDs was in the range of 3–5 nm (Figure 1d and 1e). The crystalline size calculated using Scherrer equation from XRD data was 3 nm.

Figure 1b shows the X-ray diffraction patterns of the synthesized CdTe QD nanoparticles provides information about both the crystal-structure and nanocrystalline properties. The diffraction peaks are broad and weak, but relative intense peaks at 2θ = 25°, 40°, and 47° correspond well for bulk CdTe [39]. The Raman spectrum of aqueous CdTe QDs as shown in Figure 1c ranging from 80 to 400 cm^{-1} were obtained. In low Raman shift regime between 80 to 200 cm^{-1} for CdTe QD dominated by two tellurium-related bands at wavenumbers around 121 and 141 cm^{-1} [40].

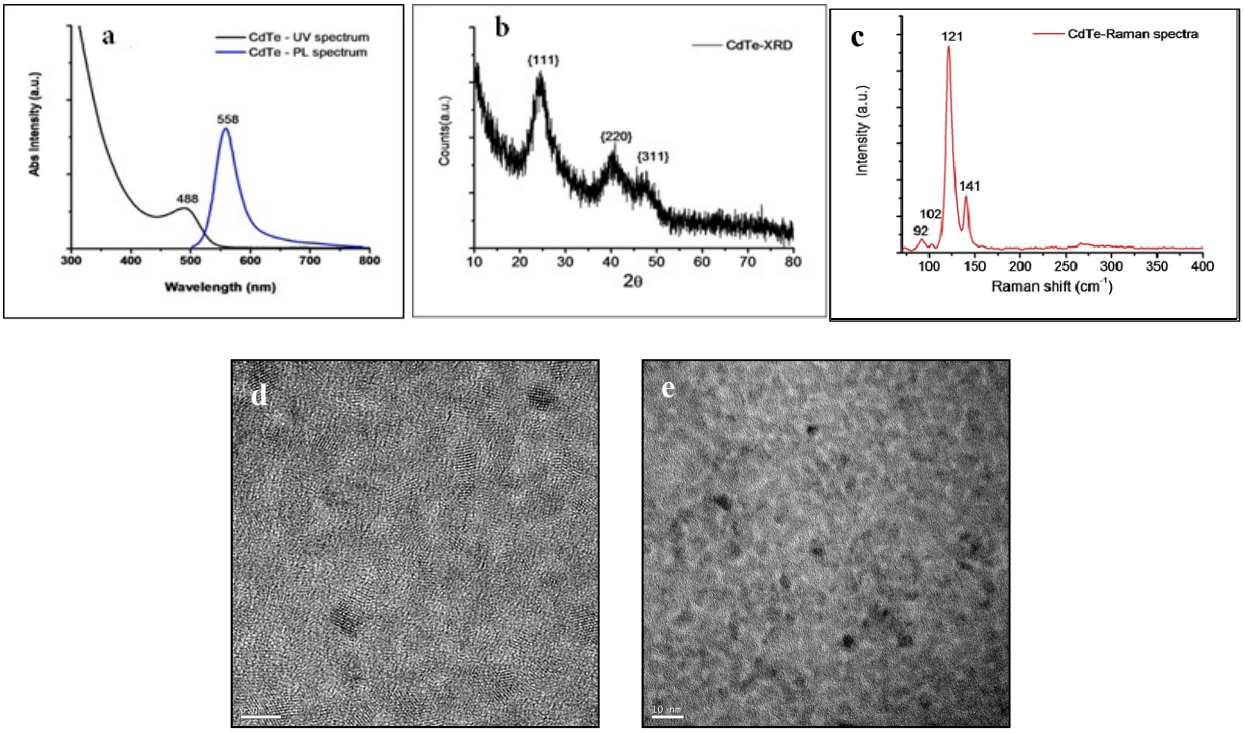

Figure 1. Characterisation of CdTe QDs by UV-Vis spectroscopy, XRD and Raman spectroscopy. (a) CdTe QDs show broad absorption peak in visible region at 488 nm and narrow emission peak at 558 nm (λ_{ex} at 488 nm), (b) X-ray diffraction pattern of CdTe QDs shows the diffraction peaks centred at 2θ = 25°, 40°, and 47°, (c) The Raman spectrum for CdTe QD dominated by two tellurium-related bands at wavenumbers around 121 and 141 cm^{-1}. (d and e) Transmission electron micrographs of CdTe quantum dots. Scale bar in d = 10 nm and e = 5 nm.

3.2. Interactions between Lysozyme and CdTe QDs

In case of lysozyme, steady decrease in the fluorescence of CdTe QDs with minor bathochromic shift from 540 nm to 545 nm was observed (Figure 2a) and steady increase in the intrinsic fluorescence without any peak shift was observed in CdTe-Lysozyme mixtures (Figure 2b). Steady decrease in the fluorescence with minor red shift indicates characteristic change in the 3D structure of lysozyme. Slight bathochromic shift in CdTe QDs fluorescence from 540 nm to 545 nm and remarkable increase in intrinsic fluorescence of QDs-lysozyme interaction at lysozyme concentration

of 4.0×10^{-6} M signifies degeneration of hydrogen bonding between alpha helices of lysozyme and possible conformational change.

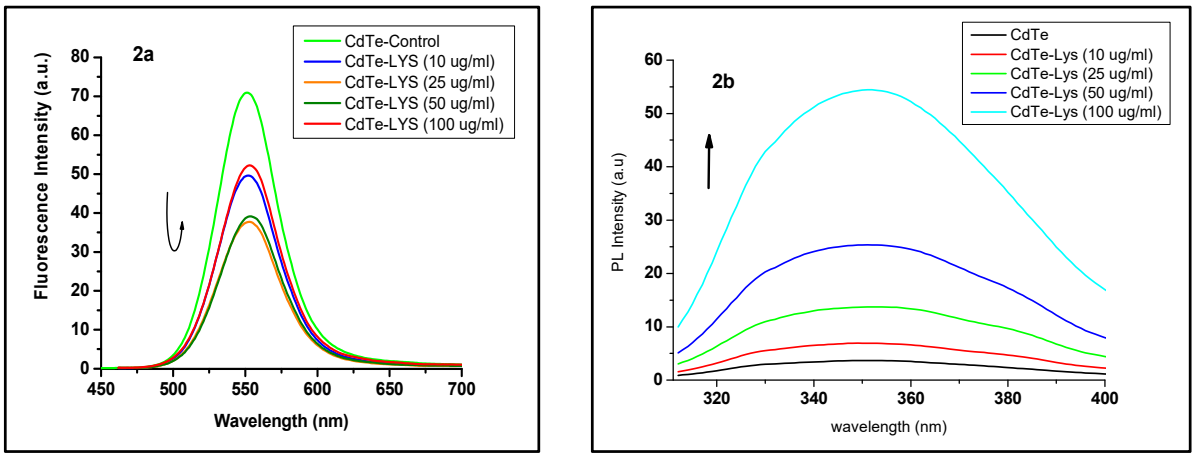

Figure 2. The electrostatic interactions of CdTe QDs with lysozyme at different concentrations. (a) shows steady decrease in fluorescence of QD with respect to increasing concentration of lysozyme, (b) shows increase in intrinsic fluorescence of lysozyme at 355 nm.

3.3. Interactions between Hemoglobin and CdTe QDs

The interactions of Hemoglobin with CdTe QDs interactions showed similar trends as observed in lysozyme-QDs interactions. The steady decrease in fluorescence of CdTe QDs with increase in Hb concentration without any peak shift was observed (Figure 3a) and linear increase in intrinsic fluorescence was observed (Figure 3b).

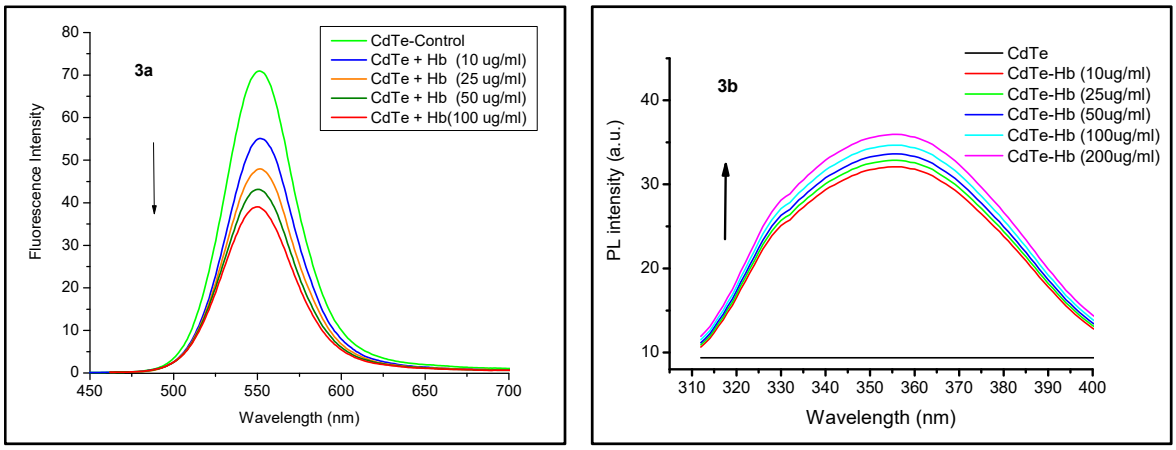

Figure 3. Physical interaction of CdTe QDs & hemoglobin at different concentration. (a) shows steady decrease in fluorescence of QD with respect to increasing concentration of hemoglobin, (b) shows increase in intrinsic fluorescence of hemoglobin at 355 nm.

3.4. Interactions between BSA and CdTe QDs

The BSA shows increase in both, the QDs fluorescence and intrinsic fluorescence of BSA (Figure 4a). The fluorescence of CdTe QDs increased linearly with increase in concentration of BSA without any peak shift in its intrinsic fluorescence (Figure 4b). The steady increase in the fluorescence CdTe QDs after interaction with BSA and intrinsic fluorescence of BSA strongly indicate that some conformational changes are occurring due to the interaction suggesting availability of more binding sites for CdTe QDs.

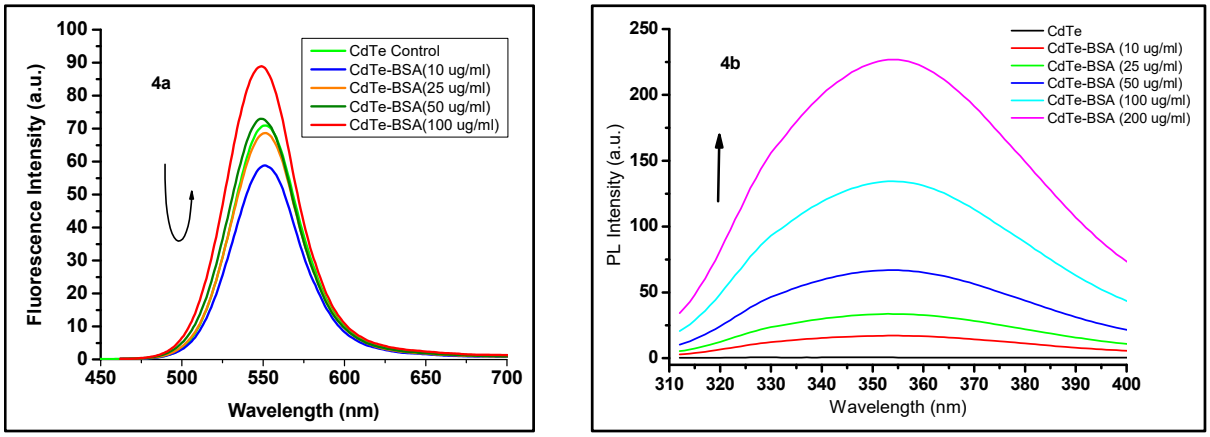

Figure 4. Physical interaction of CdTe QDs & BSA at different concentration. (a) shows steady increase in fluorescence of QD with respect to increasing concentration of BSA, (b) shows increase in intrinsic fluorescence of hemoglobin at 355 nm.

3.5. FTIR Spectrum Analysis

To study the mechanism of electrostatic interactions of CdTe QDs with proteins at different concentrations, FTIR spectra of CdTe QD-protein complex were determined. In case of CdTe QD-lysozyme, Figure 5a at lower concentrations of Lysozyme (10–50 µg/ml) FTIR spectra show the prominentpeaks at 1450 cm^{-1} pertaining to proline (71 & 103) side chain and 1724 and 1796 cm^{-1} are assigned for (C–N) amides (C=O stretching mode). With increase in concentration of Lysozyme intensity of peak at 1450 cm^{-1} was increased indicating more interactions of CdTe QDs with proline. As alpha helices are present on the outer side of the lysozyme, possibly prolines from these sites are interacting with QDs.

The Figure 5b shows the FTIR spectra of CdTe QD-Hemoglobin complex. The peaks are observed at 1446, 1722, 1796 cm^{-1} assigned to stretching vibrations of Amide (C=O stretching mode) and peak at 1651 cm^{-1} assigned for amine (–C=N– bend) [41]. At higher concentration of Hb (200 µg/ml), intense peak at 1651 cm^{-1} indicates (N–Htrans to carbonyl oxygen) Amide-II bend suggesting increased hydrogen bonding between porphyrin ring of Hb and QDs. At lower concentrations of Hb (10–100 µg/ml) FTIR spectra indicate interactions between only (C=O) amide reagion of protein & CdTe QD.

In case of CdTe QD-BSA complex, Figure 5c shows three prominent peaks at 1030 cm^{-1}, 940 cm^{-1} and 814 cm^{-1}. Peaks at 1030 cm^{-1}, 940 cm^{-1} are assigned to streching vibrations of (C–O)

Amide-I and (–COOH) side chain of serine amino acid respectively. The peak at 814 cm^{-1} is assigned to (–C–H) bend of p-substituted aromatic amino acid such as tyrosine [41,42]. Furthermore, rise in the intensity of above three mentined peaks, especially the peak at 814 cm^{-1} with the increasing concentration of BSA (from 10 to 100 µg/ml) indicate increasing contribution of serine and tyrosine to electrostatic interaction with QDs. Surprisingly, at higher concentration of BSA (200 µg/ml) peak at 814 cm^{-1} supresses remarkably shows hindered tyrosine interaction with QDs due to conformational changes in BSA. Scheme 1 depicts the locations of amino acids on respective proteins, the sites of interaction with negatively charged CdTe QDs.

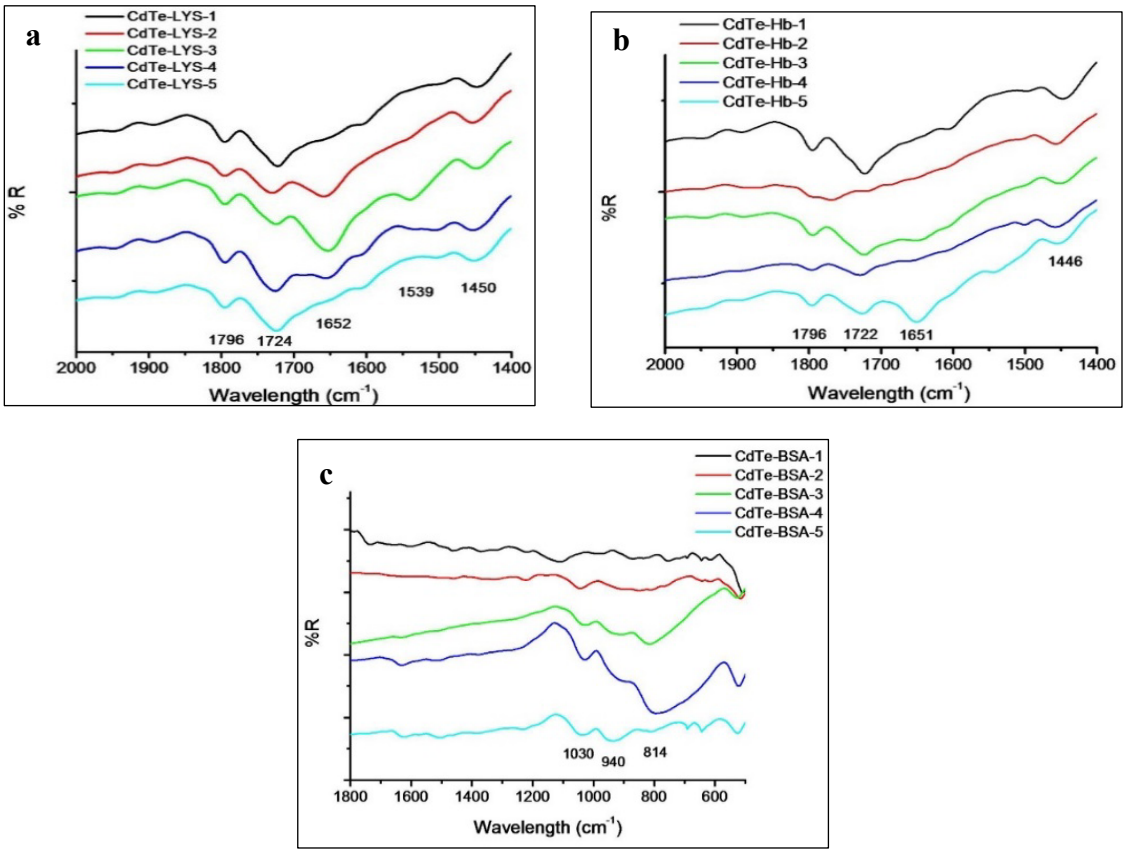

Figure 5. FTIR spectrum of CdTe QDs-Protein complex at the level of various concentrations of proteins. (a) Lysozyme [Lysozyme concentration at various levels: CdTe-Lys-1 = 0.0 µg/ml (control), CdTe-Lys-2 = 10 µg/ml, CdTe-Lys-3 = 25 µg/ml, CdTe-Lys-4 = 50 µg/ml, CdTe-Lys-5 = 100 µg/ml]. (b) Hemoglobin [Hemoglobin concentration at various levels: CdTe-Hb-1 = 0.0 µg/ml (control), CdTe-Hb-2 = 10 µg/ml, CdTe-Hb-3 = 25 µg/ml, CdTe-Hb-4 = 50 µg/ml, CdTe-Hb-5 = 100 µg/ml]. (c) BSA [BSA concentration at various levels: CdTe-BSA-1 = 0.0 µg/ml (control), CdTe-BSA-2 = 10 µg/ml, CdTe-BSA-3 = 25 µg/ml, CdTe-BSA-4 = 50 µg/ml, CdTe-BSA-5 = 100 µg/ml].

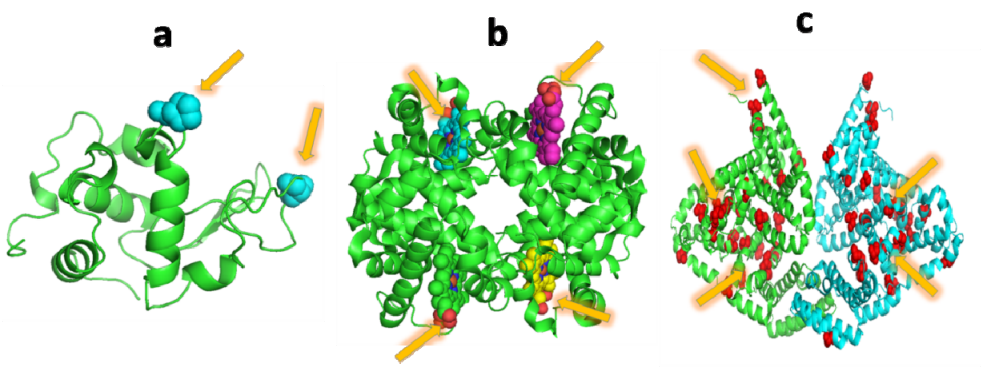

Arrows indicate the probable sites on proteins where the interaction with CdTe QDs occur. (a) Lysozyme (proline residue) , (b) Hemoglobin (Heme), (c) BSA (Serine residue)

Scheme 1. Schematic showing the locations of specific amino acids in the 3D conformation of respective proteins where the CdTe QDs interact with them.

3.6. Stern–Volmer Analysis of CdTe QD-Protein Interactions

The changes in the interactions between CdTe QDs and proteins reflect in the changes of the intrinsic fluorescence of proteins at 355 nm originating from the tryptophan (Trp) and tyrosine (Tyr) residues. These changes in the intrinsic fluorescence of proteins can be analysed by the Stern–Volmer equation and the trends of binding affinities of CdTe QDs and proteins can be understood. The observed fluorescence quenching probably arises from the energy transfer occurring between proteins and CdTe QDs. The intrinsic fluorescence of the proteins was quenched in case of lysozyme and hemoglobin and incresed gradually in BSA. The fluorescence quenching mechanism can be analyzed quantitatively at different concentrations of proteins at constant temparature with the Stern–Volmer equation.

$$\frac{F0}{F} = 1 + Ksv.[Q] \quad (1)$$

where, F_0 and F are the relative fluorescence intensities of protein at 355 nm in the absence and presence of quencher, respectively. K_{sv} is the Stern–Volmer quenching constant, and [Q] is the concentration of quencher (CdTe QDs).The Stern–Volmer plots of proteins (Lysozyme, Hb, BSA) at different concentrations.

In case of CdTe QD-Lysozyme, Figure 6a shows the linear increase in fluorescence quenching (K_q) up to the concentration of 50 µg/ml and then quenching suddenly decreased linearly up to 200 µg/ml. The increase in K_q indicates more binding affinity of lysozyme to CdTe QDs and its susceptibility to the conformational changes up to its certain concentration (10–50 µg/ml). The further increase in the concentration of lysozyme reduces the binding affinity for CdTe QDs. This may be because of steric hindrance for lysozyme at higher concentration which may be either because of saturation of CdTe QD surface or loss of co-operative binding. Figures 2a and 2b also show gradual increase in intrinsic fluorescence spectra.

However, in case of CdTe QD-Hemoglobin interaction, there was no change in K_q up to 50 µg/ml as shown in Figure 6b and then it subsequently increased than hat have seen in case of BSA and Lysozyme. Relatively unchanged fluorescence at lower concentration of Hb quenching suggests

that hemoglobin may be due to the presence of porphyrin ring in hemoglobin which imparts rigidity to the structure. Therefore, at low concentration and very rare chance of conformational change it shows stationary fluorescence quenching then at higher concentration due to structural rigidity steric hindrance may occur against acquiring electrostatic interaction with CdTe QDs because of high affinity towards them.

In case of CdTe QD-BSA, Figure 6c shows gradual decrease in K_q upto the concentration of 50 µg/ml of BSA then it suddenly increased at higher concentration of BSA (100–200 µg/ml). It also shows linear decrease in K_q to concentration 25 µg/ml. Slight change in K_q linearity from 25–50 µg/ml due to conformational changes in BSA which were also seen in fluorescence spectra of BSA (Figures 4a and 4b).

Table 1 shows Stern–Volmer equation analysis for each protein. This table represents relation between binding affinity of CdTe QDs with proteins in the terms quenching of CdTe QDs fluorescence. In case of BSA, binding constant is directly proportional to quenching constant. Upto the concentration of 25 µg/ml binding Constant (K_{sv} = 0.0264) shows gradual increase with Quenching constant also, which marks optimum concentration of CdTe QD for BSA. After that it again shows gradual decrease in binding constant (K_{sv} = −0.0261 to −0.0005) and quenching constant (K_q = −1.3 to −0.03), which may again due to conformational change in three-dimensional structure of BSA.

All three proteins show that binding constant (K_{sv}) is directly proportional to the fluorescence quenching constant (K_q). Both the proteins Lysozyme and BSA show increase in K_{sv} with CdTe QDs up to the concentration of 50 µg/ml and 25 µg/ml, respectively. At higher concentration of Lysozyme & BSA, K_{sv} decreased subsequently. In case of Hemoglobin, there is no considerable change in K_{sv} up to the concentration of 50 µg/ml, after that there is gradual increase in K_{sv} up to the concentration of 100–200 µg/ml which was also supported by UV-Vis (Figure 3a, 3b) and Stern–Volmer analysis (Figure 6b).

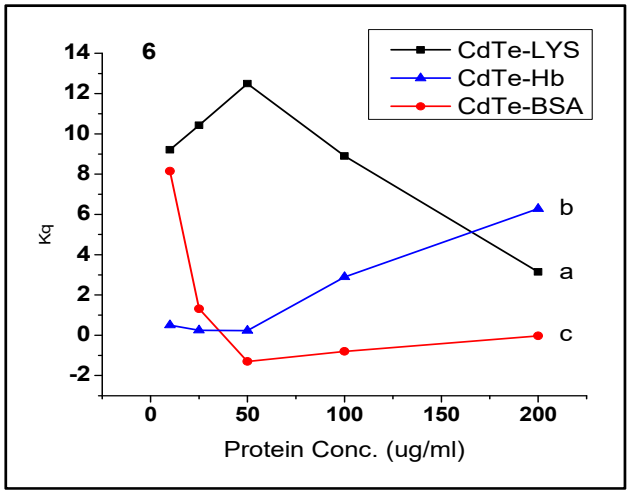

Figure 6. Stern–Volmer equation analysis of each protein. The figure shows the ratio of relative fluorescence intensities (F_0/F) versus concentration of proteins, (a) BSA, (b) Lysozyme, (c) Hemoglobin.

Table 1. Stern–Volmer equation analysis for each protein. K_{sv} represents relation between physical binding of CdTe QDs with proteins which get result into quenching K_q of CdTe QDs fluorescence.

Sr. No.	NP-Biomolecule Complex (Conc. Of Protein)	Binding Constant K_{sv} ($a \times 10^6$)			Quenching Constant K_q ($b \times 10^{12}$)		
		CdTe-Lys	CdTe-BSA	CdTe-Hb	CdTe-Lys	CdTe-BSA	CdTe-Hb
1	10 µg/ml	0.182	0.163	0.003	9.21	8.15	0.5
2	25 µg/ml	0.208	0.0264	0.005	10.43	1.32	0.25
3	50 µg/ml	0.250	−0.0261	0.007	12.5	−1.30	0.23
4	100 µg/ml	0.179	−0.0179	0.009	8.90	−0.80	2.90
5	200 µg/ml	0.063	−0.0005	0.012	3.15	−0.03	6.28

3.7. Analysis of Raman Spectra

Figure 7 shows Raman spectra of individual CdTe QD-protein complex (He-Ne laser λ_{ex} = 632.8 nm). As shown in the Figure 7a, in CdTe QD-BSA complex, peaks at 1650–1660 cm^{-1} band regions belong to contribution from amide bond (CO–NH), which is characteristic of high α-helical content in BSA. The 1002 cm^{-1} band region related to the phenylalanine and 1340–1350 cm^{-1} band region related to tryptophan or C–H bending.

In case of CdTe QD-Hemoglobin complex in Figure 7b peaks in the region of 150–600 cm^{-1} characterized by the stretching modes of the Fe ligand bonds and peaks in the region of 600–1200 cm^{-1} assigned to pyrrole vibrations, 1300–1400 cm^{-1} region called oxidation state marker band region, 1650–1500 cm^{-1} region: called core size or spin state marker band region.

These results indicate that each protein interacts specifically with CdTe at the nanoparticle-protein interface. This is significant for the understanding of how nanoparticle-protein interactions will influence their respective physicochemical properties.

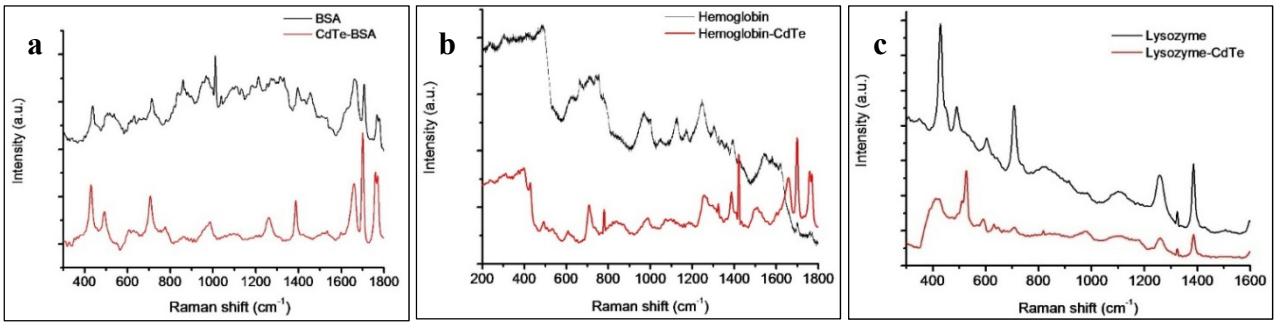

Figure 7. Raman spectra of individual proteins and protein-Quantum dots interactions. (a) BSA and BSA-CdTe QDs, (b) Hemoglobin and hemoglobin-CdTe QDs, (c) Lysozyme and Lysozyme-CdTe QDs.

4. Conclusion

In summary, all three proteins, Lysozyme, BSA and Hemoglobin which belong to non-globular, globular and metalloprotein families respectively interact differently with CdTe quantum dots. For these three proteins, a general trend was observed in case of Lysozyme and BSA that at protein concentrations from 10 μg/ml to 200 μg/ml, binding affinity (K_{sv}) to CdTe QDs is directly proportional to quenching constant (K_q). Amongst relative change in binding affinity (K_{sv}) of proteins to CdTe QDs is highest in case of BSA & lowest in case of Hemoglobin.

All three proteins have different electrostatic interactions with CdTe QDs reflecting in different binding and quenching constants. Moreover, the concentration of the protein also has the influence on the protein-CdTe QD interactions. We believe that this anomalous fluorescence quenching behavior of all three proteins studied here resembles characteristic three dimensional structures and rigidity of respective proteins and the mechanism of QDs interaction. According to fluorescence spectra and Stern–Volmer equation, among three proteins BSA is structurally unstable after interaction with CdTe QDs and Hemoglobin is most structurally stable due to its rigid porphyrin ring structure. In case of Hemoglobin-CdTe QDs interaction, we predict that due to its rigid porphyrin ring structure, there was no change in the fluorescence quenching up to the concentration of 50 μg/ml. After that the sudden rise in quenching suggests conformational change in three-dimensional structure of the protein in such way that more binding sites became available for interaction with CdTe QDs resulting in the increase in fluorescence quenching. Similarly, in case of Lysozyme and BSA, which consist of alpha helices as a major constituent in three-dimensional structure of protein, the conformation may change at a particular concentration and thereafter a significant drop in fluorescence quenching was observed.

In conclusion, this study reflects that nanoparticle-protein interactions depend not only on the surface chemistry of the nanoparticle but also on the protein structure. Each globular, metalloprotein and non-globular proteins interact differently and have variable effects on the fluorescence property of the Quantum dots. At the same time the intrinsic fluorescence of the proteinsis also influenced. The understanding of these interactions is important for in-vitro and in-vivo applications of Quantum dots in the field of biomedical and bioengineering research and advanced biological applications.

Acknowledgements

AK gratefully acknowledges the funding support from Nano mission, Department of Science and Technology, India. AK is also thankful for the support given by Dr. Satishchandra Ogale, National Chemical Laboratory for characterization of nanomaterials.

Conflict of Interest

The authors declare that there is no conflict of interest regarding the publication of this manuscript.

References

1. Alivisatos AP (1996) Perspectives on the Physical Chemistry of Semiconductor Nanocrystals. *J Phys Chem* 100: 13226–13239.
2. Zhong X, Feng Y, Knoll W, et al. (2003) Alloyed $Zn_xCd_{1-x}S$ Nanocrystals with Highly Narrow Luminescence Spectral Width. *J Am Chem Soc* 125: 13559–13563.
3. Abd El-sadek MS, Moorthy Babu S (2010) Growth and optical characterization of colloidal CdTe nanoparticles capped by a bifunctional molecule. *Physica B* 405: 3279–3283.
4. Bruchez Jr M, Moronne M, Gin P, et al. (1998) Semiconductor nanocrystals as fluorescent biological labels. *Science* 281: 2013–2016.
5. Chan WC, Nie S (1998) Quantum dot bioconjugates for ultrasensitive nonisotopic detection. *Science* 281: 2016–2018.
6. Wu F, Lewis JW, Kliger DS, et al. (2003) Unusual excitation intensity dependence of fluorescence of CdTe nanoparticles. *J Chem Phys* 118: 12–16.
7. Wu X, Liu H, Liu J, et al. (2003) Immunofluorescent labeling of cancer marker Her2 and other cellular targets with semiconductor quantum dots. *Nat Biotechnol* 21: 41–46.
8. Han M, Gao X, Su JZ, et al. (2001) Quantum-dot-tagged microbeads for multiplexed optical coding of biomolecules. *Nat Biotechnol* 19: 631–635.
9. Sahoo SK, Labhasetwar V (2003) Nanotech approaches to drug delivery and imaging. *Drug Discov Today* 8: 1112–1120.
10. Wang Y, Zheng J, Zhang Z, et al. (2009) CdTe nanocrystals as luminescent probes for detecting ATP, folic acid and l-cysteine in aqueous solution. *Colloid Surface A* 342: 102–106.
11. Goldman ER, Clapp AR, Anderson GP, et al. (2004) Multiplexed toxin analysis using four colors of quantum dot fluororeagents. *Anal Chem* 76: 684–688.
12. Gerion D, Parak WJ, Williams SC, et al. (2002) Sorting fluorescent nanocrystals with DNA. *J Am Chem Soc* 124: 7070–7074.
13. Mamedova NN, Kotov NA, Rogach AL, et al. (2001) Albumin-CdTe Nanoparticle Bioconjugates: Preparation, Structure, and Interunit Energy Transfer with Antenna Effect. *Nano Lett* 1: 281–286.
14. Yamasaki K, Maruyama T, Kragh-Hansen U, et al. (1996) Characterization of site I on human serum albumin: concept about the structure of a drug binding site. *BBA-Protein Struct Mol Enzymol* 1295: 147–157.
15. Medintz IL, Uyeda HT, Goldman ER, et al. (2005) Quantum dot bioconjugates for imaging, labelling and sensing. *Nat Mater* 4: 435–446.
16. Liu C, Bo A, Cheng G, et al. (1998) Characterization of the structural and functional changes of hemoglobin in dimethyl sulfoxide by spectroscopic techniques. *BBA-Protein Struct Mol Enzymol* 1385: 53–60.
17. De S, Girigoswami A (2006) A fluorimetric and circular dichroism study of hemoglobin—Effect of pH and anionic amphiphiles. *J Colloid Interf Sci* 296: 324–331.
18. Cheng Y, Lin H, Xue D, et al. (2001) Lanthanide ions induce hydrolysis of hemoglobin-bound 2,3-diphosphoglycerate (2,3-DPG), conformational changes of globin and bidirectional changes of 2,3-DPG-hemoglobin's oxygen affinity. *BBA-Mol Basis Dis* 1535: 200–216.
19. Sil S, Kar M, Chakraborti AS (1997) Studies on the interaction of hematoporphyrin with hemoglobin. *J Photoch Photobio B* 41: 67–72.

20. Kondo A, Mihara J (1996) Comparison of Adsorption and Conformation of Hemoglobin and Myoglobin on Various Inorganic Ultrafine Particles. *J Colloid Interf Sci* 177: 214–221.
21. Kondo A, Fukuda H (1998) Effects of Adsorption Conditions on Kinetics of Protein Adsorption and Conformational Changes at Ultrafine Silica Particles. *J Colloid Interf Sci* 198: 34–41.
22. Teraoka J, Bell A (1998) Loop structure in Human serum albumin from Raman optical activity. *J Raman Spectrosc* 19: 67–71.
23. Liang J, Cheng Y, Han H (2008) Study on the interaction between bovine serum albumin and CdTe quantum dots with spectroscopic techniques. *J Mol Struct* 892: 116–120.
24. Brewer SH, Glomm WR, Johnson MC, et al. (2005) Probing BSA binding to citrate-coated gold nanoparticles and surfaces. *Langmuir* 21: 9303–9307.
25. Lundqvist M, Sethson I, Jonsson BH (2004) Protein adsorption onto silica nanoparticles: conformational changes depend on the particles' curvature and the protein stability. *Langmuir* 20: 10639–10647.
26. Zhisong Lu, Weihua Hu, et al. (2011) Interaction mechanisms of CdTe quantum dots with proteins possessing different isoelectric points. *Med Chem Commun* 2: 283–286.
27. Gao X, Chan WCW, Nie S (2002) Quantum-dot nanocrystals for ultrasensitive biological labeling and multicolor optical encoding. *J Biomed Opt* 7: 532–537.
28. Liang JG, Ai XP, He ZK, et al. (2004) Functionalized CdSe quantum dots as selective silver ion chemodosimeter. *Analyst* 129: 619–622.
29. Wang JH, Wang HQ, Zhang HL, et al. (2007) Purification of denatured bovine serum albumin coated CdTe quantum dots for sensitive detection of silver(I) ions. *Anal Bioanal Chem* 388: 969–974.
30. Willard DM, Carillo LL, Jung J, et al. (2001) CdSe-ZnS Quantum Dots as Resonance Energy Transfer Donors in a Model Protein-Protein Binding Assay. *Nano Lett* 1: 469–474.
31. Huang X, Li L, Qian H, et al. (2006) A Resonance Energy Transfer between Chemiluminescent Donors and Luminescent Quantum-Dots as Acceptors (CRET). *Angew Chem Int Edit* 45: 5140–5143.
32. Gu Z, Zhu X, Ni S, et al. (2004) Conformational changes of lysozyme refolding intermediates and implications for aggregation and renaturation. *J Biochem Cell Biol* 36: 795–805.
33. Yang F, Liang Y (2003) Unfolding of Lysozyme Induced by Urea and Guanidine Hydrochloride Studied by "Phase Diagram" Method of Fluorescence. *Acta Chim Sinica* 61: 803–807.
34. Chandra G, Ghosh KS, Dasgupta S, et al. (2010) Evidence of conformational changes in adsorbed lysozyme molecule on silver colloids. *Int J Biol Macromol* 47: 361–365.
35. Yang T, Li Z, Wang L, et al. (2007) Synthesis, Characterization, and Self-Assembly of Protein Lysozyme Monolayer-Stabilized Gold Nanoparticles. *Langmuir* 23: 10533–10538.
36. Wu YL, He F, He XW, et al. (2008) Spectroscopic studies on the interaction between CdTe nanoparticles and lysozyme. *Spectrochim Acta A* 71: 1199–1203.
37. Sanfins E, Dairou J, Rodrigues-Lima F, et al. (2011) Nanoparticle-protein interactions: from crucial plasma proteins to key enzymes. *J Phys: Conference Series* 304: 012039.
38. Anup K, Sonia K, Prasad Y, et al. (2011) Magnetite/CdTe magnetic-fluorescent composite nanosystem for magnetic separation and bio-imaging. *Nanotechnology* 22: 225101.
39. Idowu M, Lamprecht E, Nyokong T (2008) Interaction of water-soluble thiol capped CdTe quantum dots and bovine serum albumin. *J Photoch Photobio A* 198: 7–12.

40. Rakovich YP, Gerlach M, Donegan JF, et al. (2005) Three-dimensional photon confinement in a spherical microcavity with CdTe quantum dots: Raman spectroscopy. *Physica E* 26: 28–32.
41. Barth A (2007) Infrared spectroscopy of proteins. *BBA-Bioenergetics* 1767: 1073–1101.
42. Barth A, Zscherp C (2002) What vibrations tell about proteins. *Q Rev Biophys* 35: 369–430.

AIMS Press